Synthesis and iron(III) complexing ability of CacCAM, a new analog of enterobactin possessing a free carboxylic anchor arm. Comparative studies with TRENCAM

Daniel Imbert,[a] Fabrice Thomas,[a] Paul Baret,[a] Guy Serratrice,[a] Didier Gaude,[a] Jean-Louis Pierre*[a] and Jean-Pierre Laulhère[b]

[a] *Laboratoire de Chimie Biomimétique (LEDSS, CNRS UMR 5616) Université J. Fourier, BP 53, 38041 Grenoble cedex 9, France. E-mail: Jean-Louis.Pierre@ujf-grenoble.fr*
[b] *CBCRB, DBMS/CB, CEA Grenoble, 17 av. des Martyrs, 38054 Grenoble cedex 9, France*

Received (in Strasbourg, France) 29th December 1999, Accepted 18th February 2000
Published on the Web 13th April 2000

A new tricatecholate, CacCAM, has been synthesized by attachment of three catecholamide subunits to a CO_2H-functionalized triamine backbone. The solution coordination chemistry of the ligand and its iron(III) complex have been investigated by potentiometric, spectroscopic and kinetic methods. The results are compared to those obtained with TRENCAM, which possesses the same catecholamide subunits, but a TREN [tris(2-aminoethyl)-amine] backbone. The stability constant ($\log \beta_{110} = 42.9$, $pFe = 27.5$) is close to that of TRENCAM ($\log \beta_{110} = 43.6$, $pFe = 27.8$), showing that a change of backbone does not significantly alter the iron chelating ability of the ligand. Kinetics of iron exchange between Fe(III)–EDTA and CacCAM or TRENCAM involves similar rate constants (16 ± 1 and 14 ± 2 M^{-1} s^{-1}, respectively). EPR data show that the iron(III) does not have the same distorted rhombic geometry in the two complexes. Fe(III)–CacCAM has been tested as a source of iron in nutritional experiments with *Arabidopsis thaliana* plant cells: its efficiency is good, comparable to that of Fe(III)–EDTA, the most widely used iron complex for plant nutrition.

Introduction

Most living organisms require iron for their growth. Siderophores are low molecular weight iron(III) chelators excreted by microorganisms for the uptake of iron.[1] Interest in synthetic biomimetic siderophores includes: (*i*) their potential applications as clinical iron removal agents (iron overload is one of the most common types of poisoning),[2] (*ii*) the use of their iron complexes in agriculture for prevention or treatment of chlorosis[3] and (*iii*) their design as structural probes and diagnostic tools.[4] Siderophores typically contain three catecholate or three hydroxamate groups to bind[2] a ferric ion, giving octahedral complexes. For most applications the synthetic siderophore (usully a tripodal derivative bearing one bidentate ligand on each arm) and its iron complex have to be water-soluble and, to achieve this, numerous abiotic iron chelators are derivatized with three sulfonate groups.[5] The sulfonation strategy leads to highly hydrophilic chelators and complexes, unable to cross over lipophilic membranes.[6]

On the other hand, the interest in grafted iron chelators (analytical applications, biomedical applications with control of the hydrophilic/lipophilic balance) or in fluorescent labeled siderophore analogs involves the design of new ligands. Syntheses of tripodal precursors bearing on the C_3 axis of the ligand a functionalized anchor group, thus allowing a connection with any desired substituent, seems to be a promising strategy previously used by Shanzer and Libman.[4] TRENCAM, previously described by Raymond *et al.*,[7] and its sulfonated derivative TRENCAMS,[8] which are analogs of the natural triscatechol derivative enterobactin, are among the most powerful synthetic iron chelators. TRENCAM(S) are built by connecting three catechol subunits to a TREN central organizing unit (spacer), *via* amide linkers (Scheme 1). The substitution of the TREN unit by a C-functionalized tripodal spacer necessarily induces geometrical changes and thus may involve a different (and undesirable) iron complexing ability.

In this paper we present the synthesis, the iron complexing and iron nutritional properties towards plant cells of a new iron chelator, CacCAM (Scheme 1). CacCAM bears a free carboxylic group that is located out of the coordination sphere of the three catechol subunits. It uses the new tripodal spacer depicted in Scheme 1 (insert). CacCAM may be considered as the starting species for a series of chelators possessing exactly the same coordination sphere; thus it is important to characterize the iron complexing abilities of CacCAM.

Results and discussion

Synthesis

The synthetic pathway is depicted on Schemes 2 and 3. The protected 2,3-hydroxybenzoic acid is activated with thionyl chloride and coupled with **5** in order to obtain **6**. Then, three steps are needed to obtain protected CacCAM, **9**. Deprotection of **9** gives CacCAM, **10**. The key synthon **5** has been obtained in five steps with a global yield of 30% from the starting commercial reagents.

Ligand deprotonation constants

CacCAM possesses seven deprotonation sites (six phenolic and one carboxylic groups) and is denoted LH_7. The potentiometric titration of the fully protonated ligand with NaOH

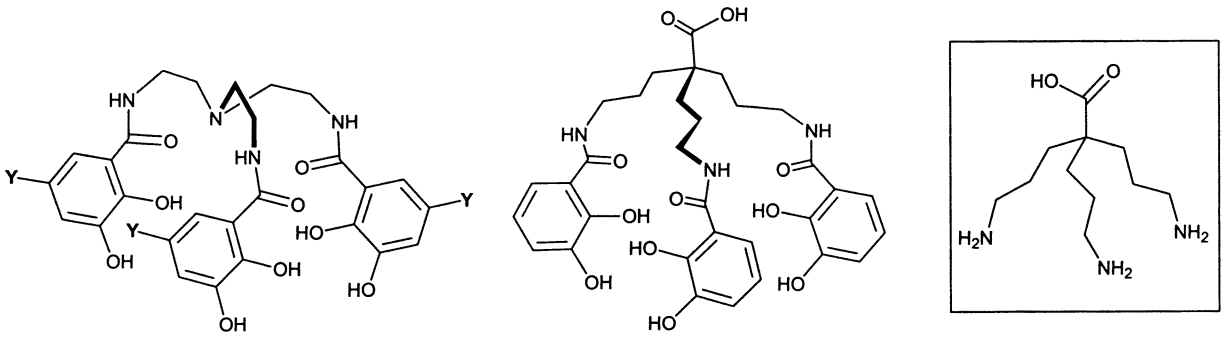

Scheme 1

in 0.1 M $NaClO_4$ at 25 °C (Fig. 1, curve a) allowed the determination of only three deprotonation constants of the catechol groups. The precipitation of the ligand below pH 5 (neutral LH_7 species) precludes the use of these data in the refinement program. Hence, the lowest pK_a corresponding to the deprotonation of the carboxyl (pK_{a_7}) cannot be determined ($pK_a < 5$). Analysis of the potentiometric titration curve over the pH range 6–10.6 by the SUPERQUAD[9] program yielded the pK_{a_n} values (106 points, $\sigma_{fit} = 2.2$, $pK_{a_6} = 7.19 \pm 0.01$, $pK_{a_5} = 7.98 \pm 0.01$, $pK_{a_4} = 8.64 \pm 0.01$) defined by eqns. (1) and (2). Charges of complexes are omitted for sake of clarity all along the text [see also eqns. (3), (4) and (9)].

$$LH_n \rightleftharpoons LH_{n-1} + H^+ \quad (1)$$

$$K_{a_n} = [LH_{n-1}][H^+]/[LH_n] \quad (2)$$

These three pK_a values reflect a roughly statistical separation (log 3 or 0.48), which is consistent with non-interacting arms. The average of these deprotonation constants is 7.94, which is between the deprotonation constant, $pK_a = 8.42$ of *N*,*N*-dimethyl-2,3-dihydroxybenzamide[10] and the average of the deprotonation constants, $pK_a \approx 7.4$, of triscatechol ligands (TRENCAM,[7] MECAM and derivatives)[11,12] and enterobactin.[11] The lowest pK_a of the hydroxy group is roughly one unit higher for CacCAM than that for triscatechol ligands (5.6 for TRENCAM,[7] 5.9 for MECAM,[11] 6.2 for MMECAM[12]). This may be ascribed to an H-bond between the deprotonated carboxylate oxygen and the hydroxy group of the catechol.

The three higher pK_a values of the catechol groups cannot be accurately determined from potentiometric titrations, since deprotonation of these groups occurs at pH > 11. A spectrophotometric titration was carried out over the pH range 10–12. The corresponding UV spectra exhibited isosbestic points at $\lambda = 209$, 317 and 347 nm, indicating the presence of only two absorbing species (Fig. 2). The data were processed by the LETAGROP SPEFO[13,14] program (absorbance values at 10 wavelengths). The best fit [$\Sigma(A_{exp} - A_{calc})^2 = 2 \times 10^{-2}$] was obtained by considering a single proton step for the deprotonation equilibrium, yielding a pK_a value of 11.16 ± 0.02. This value is close to that obtained for TRENCAM[7] (11.26 ± 0.02). The two higher pK_a values cannot be obtained since oxidation of the catechol is observed above pH 12. These pK_a values can be assumed to be close to those (12.9 and 12.1) used for TRENCAM[7] and enterobactin.[11]

Stability constants of the ferric complexes

The equilibria of the metal complexes were studied by potentiometric and spectrophotometric titrations. The potentiometric equilibrium curve of Fe(III)–CacCAM (Fig. 1 curve b) shows a large pH jump at $m = 7$, indicating that the protons of the six catechol and of the carboxyl group are released when the ligand binds to ferric ion at pH 7.5. The precipitation of the complex under experimental conditions (0.3 mM) below pH 6.5 precluded the use of the titration data in the refinement software. A spectrophotometric titration of the ferric complex (0.09 mM) of CacCAM (Fig. 3) has been carried out from pH 8.44 to 4.65. At pH below 4.5 precipitation occurred. Between pH 8.44 and 5.69 [Fig. 3(A)] the spectra display an isosbestic point at 552 nm and a band in the visible range corresponding to a LMCT; its wavelength evolved from 495 (pH 8.44) to 519 nm (pH 5.69). Decreasing the pH from 5.43 to 4.65 resulted in the appearance of a new isosbestic

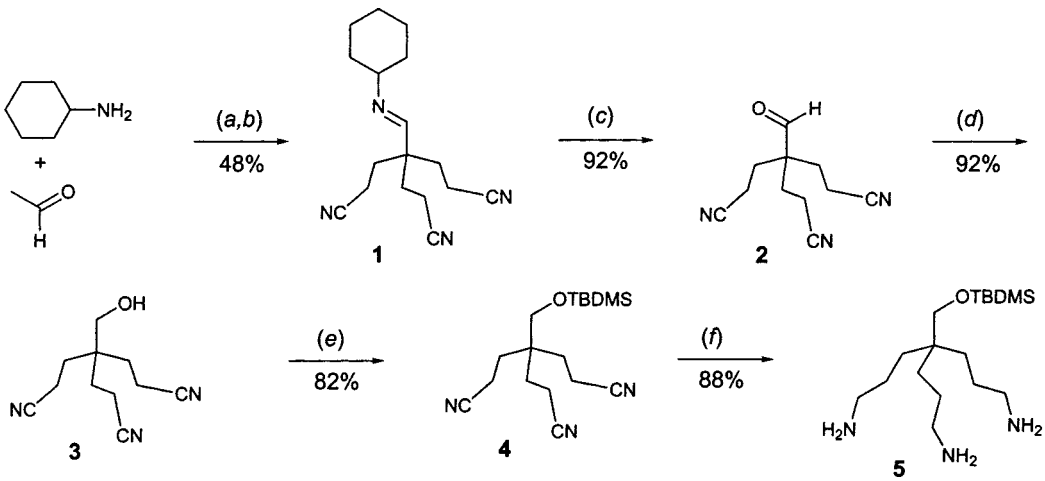

Scheme 2 (*a*) K_2CO_3, toluene, 0 °C; (*b*) acrylonitrile, 4 h, 170 °C; (*c*) HCl–H_2O, reflux; (*d*) $NaBH_4$, methanol under N_2; (*e*) TBDMSCl, DMAP, Et_3N, CH_2Cl_2 under N_2; (*f*) Raney nickel, hydrazine, ethanol.

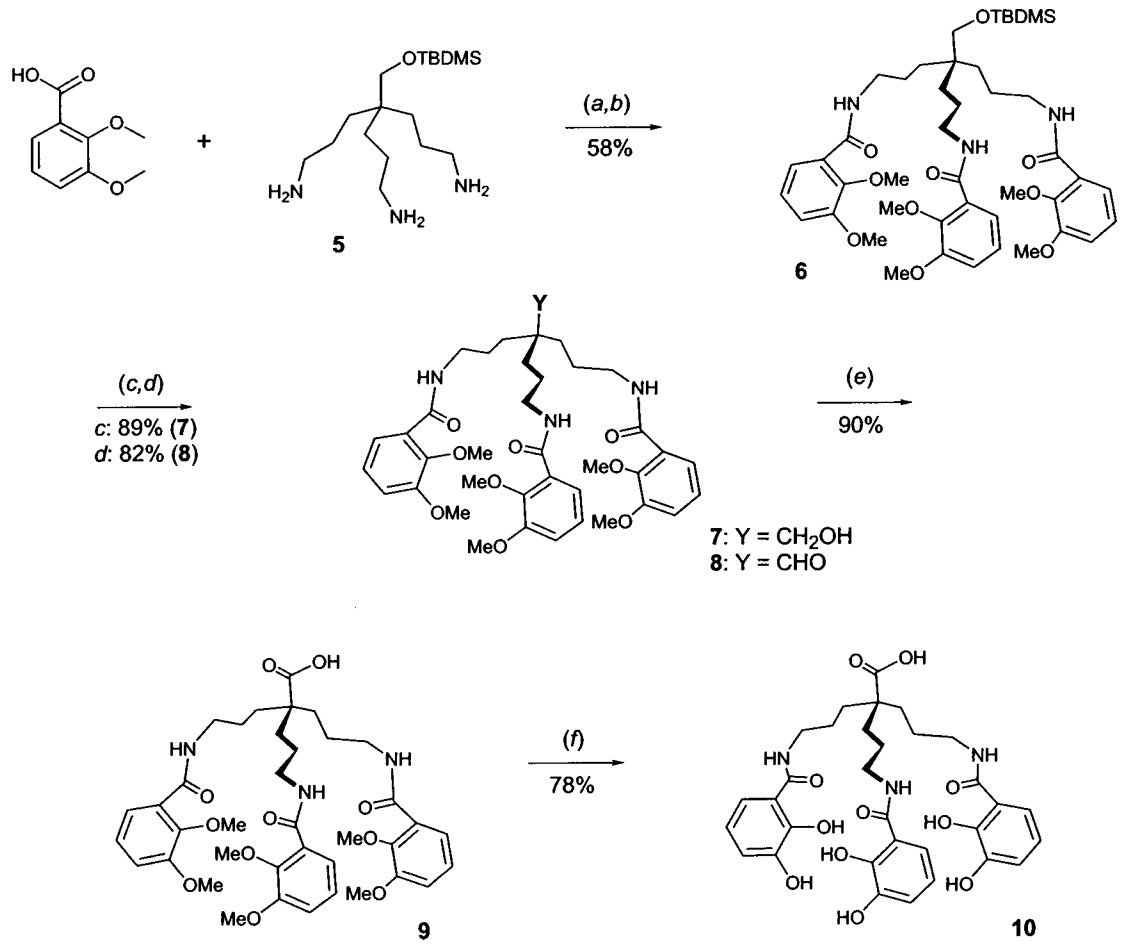

Scheme 3 (*a*) Thionyl chloride; (*b*) Et_3N, CH_2Cl_2 under N_2; (*c*) TBAF, THF; (*d*) oxalyl chloride, DMSO, CH_2Cl_2, Et_3N; (*e*) sulfamic acid, $NaClO_2$, THF–H_2O; (*f*) BBr_3, CH_2Cl_2, 0 °C.

point at 620 nm, while λ_{max} evolved from 519 to 531 nm [Fig. 3(B)]. These absorbance data were refined with the nonlinear least squares program LETAGROP SPEFO. The best refinement [$\Sigma(A_{exp} - A_{calc})^2 = 10^{-3}$] was obtained with the model including three species: $[FeL]^{4-}$, $[FeLH]^{3-}$, $[FeLH_2]^{2-}$. The calculated spectra are depicted in Fig. 4. The deprotonation constants pK_{FeLH_n} values obtained for the equilibria (3)

$$FeLH_n \rightleftharpoons FeLH_{n-1} + H^+ \quad (3)$$

are $pK_{FeLH_2} = 5.15 \pm 0.16$ and $pK_{FeLH} = 6.59 \pm 0.08$. The species distribution curves are shown in Fig. 5.

The stability constant β_{110} of the ferric complex FeL was determined by spectrophotometric competition experiments with a 1 to 200-fold excess of EDTA (denoted as Y), over the pH range 6.81 to 6.62. The competition equilibrium can be expressed by the following equations:

$$FeL + YH + 5H^+ \rightleftharpoons FeY + LH_6 \quad (4)$$

$$K = [FeY][LH_6]/[FeL][YH][H^+]^5$$

$$= \beta_{110(FeY)}K'_{a_1}/\beta_{110(FeL)}K_{a_1}K_{a_2}K_{a_3}K_{a_4}K_{a_5}K_{a_6} \quad (5)$$

where LH_6 represents the ligand CacCAM with a deprotonated carboxylic group, K_{a_1}–K_{a_6} the deprotonation constants of

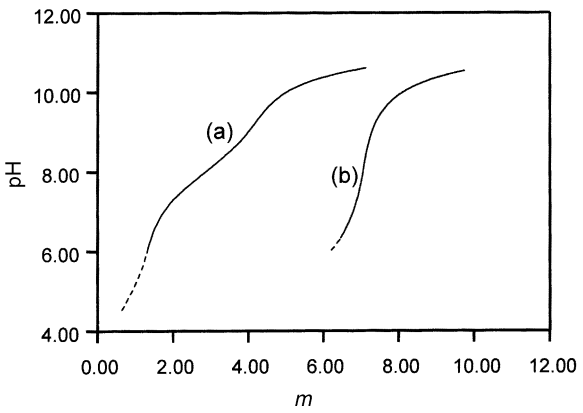

Fig. 1 Potentiometric titration curves for (a) ligand CacCAM, (b) 1 : 1 CacCAM + Fe(III); m = mole of base added per mole of ligand. [CacCAM] = 0.32 mM, T = 25 °C, I = 0.1 M ($NaClO_4$), 2% MeOH by volume. The dashed lines indicate precipitation.

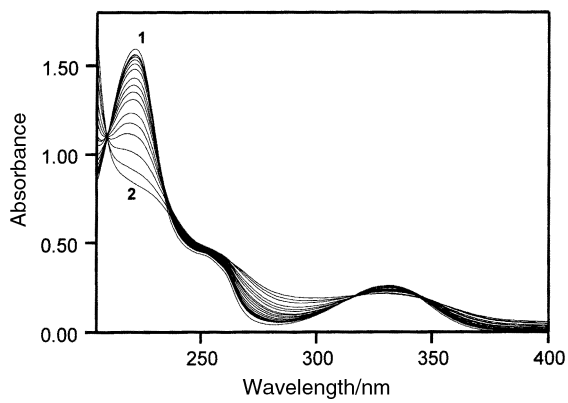

Fig. 2 UV–visible absorption spectra of CacCAM as a function of pH: [CacCAM] = 0.02 mM, I = 0.1 M ($NaClO_4$), 2% MeOH by volume. Curve 1 (pH 8.44), curve 2 (pH 11.1).

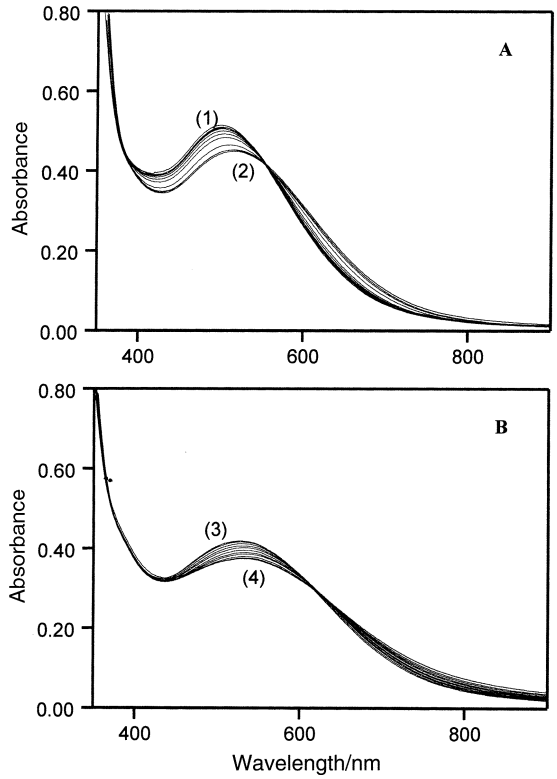

Fig. 3 UV–visible absorption spectra of Fe(III)–CacCAM as a function of pH: [CacCAM] = 0.09 mM, [Fe] = 0.09 mM, I = 0.1 M ($NaClO_4$). (A) Curve 1 (pH 8.44), curve 2 (pH 5.69); (B) curve 3 (pH 5.43), curve 4 (pH 4.65).

LH_6 and K'_{a_1} the deprotonation constant of HY ($10^{-10.2}$).[15] The concentration of FeL was calculated from the absorbance at 500 nm where FeL is the only absorbing species. The concentrations of the other species in eqns. (4) and (5) were calculated from the mass balance equation and pH:

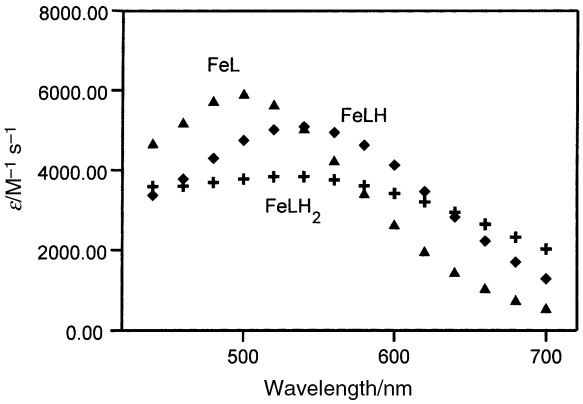

Fig. 4 Calculated extinction coefficient spectra of Fe(III)–CacCAM complexes: [CacCAM] = 0.09 mM, [Fe] = 0.09 mM, I = 0.1 M ($NaClO_4$).

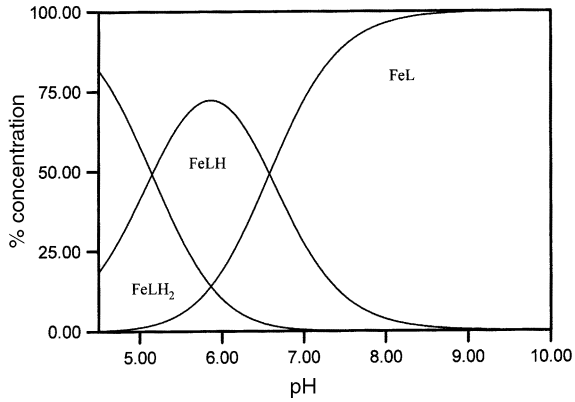

Fig. 5 Species distribution curves for Fe(III)–CacCAM from pH 4.5 to 10: [CacCAM] = [Fe^{3+}] = 1 mM.

$$[Fe]_{tot} = \beta_{FeL}[FeL] + \alpha_{FeY}[FeY] \quad (6)$$

$$[L]_{tot} = \beta_{FeL}[FeL] + \alpha_{L}[L] \quad (7)$$

$$[Y]_{tot} = \beta_{FeY}[FeY] + \alpha_{Y}[Y] \quad (8)$$

where the α are the usual Ringbom coefficients.[16] Using the known formation constant of FeY (log β_{110} = 25.1),[15] the average formation constant of the ferric CacCAM was determined to be log β_{110} = 42.5(3). To measure the efficiency of the ligand CacCAM for iron(III) at physiological pH we have calculated the concentration of free Fe^{3+} under standard conditions (pH = 7.4, $[L]_{tot} = 10^{-5}$ M, $[Fe]_{tot} = 10^{-6}$ M), which is expressed as pFe (pFe = $-\log [Fe^{3+}]$). The obtained value for CacCAM is 27.5, which is very close to that of TRENCAM (27.8).[7] The substitution of the TREN [$(N(CH_2CH_2)_3$] for the Cac [$HO_2CC(CH_2CH_2CH_2)_3$] backbone does not change significantly the complexing efficiency of the ligand.

The visible spectrum of the FeL species (λ_{max} = 495 nm) is similar to that of the iron complexes of triscatecholate ligands or of enterobactin (Table 1). However, the extinction coefficient (5900 M^{-1} cm^{-1}) is higher than that generally measured for other triscatecholate complexes (4900 M^{-1} cm^{-1}) but close to that of the ferric enterobactin (5700 M^{-1} cm^{-1})[11] and the ferric MECAMS (5900 M^{-1} cm^{-1}).[17] The UV–visible spectra of $[FeLH]^{3-}$ and $[FeLH_2]^{2-}$ species exhibited shifts in λ_{max} from 495 (pH 8.44) to 519 (pH 5.69) and 531 nm (pH 4.65). Similar shifts have been observed for catecholate complexes and have been attributed to a change from a catecholate coordination mode to a salicylate coordination mode (coordination by one hydroxyl and *O*-amide for each arm of the tripodal ligand) induced by stepwise protonations of the *m*-hydroxy groups, that is a mono-salicylate, bis-catecholate coordination in $[FeLH]^{3-}$ and a mono-chatecholate, bis-

Table 1 Equilibrium constants and UV–visible spectral characteristics of ferric complexes with triscatechol ligands

					λ_{max}/nm ($\varepsilon/10^3$ M^{-1} cm^{-1})		
Ligand	pK_{FeLH_2}	pK_{FeLH}	log β_{110}	pFe	FeL	FeLH	$FeLH_2$
CacCAM	5.15	6.59	42.5	27.5	495(5.9)	519(5.0)	531(4.0)
TRENCAM[a]	—	5.59	43.2	27.8	496(4.9)	510(4.1)	—
TRENCAMS[b]	4.2	5.5	41.3	29.6	488(5.3)	500(4.6)	—
MECAM[c]	6.03	7.2	43	29.4	492(4.7)	515(3.9)	—
MECAMS[d]	4.10	5.74	41	29.4	485(5.9)	490(5.1)	—
Enterobactin[c]	3.52	4.95	49	35.5	498(5.7)	514(4.6)	518(3.5)

[a] Ref. 7. [b] Ref. 8. [c] Ref. 11. [d] Ref. 17.

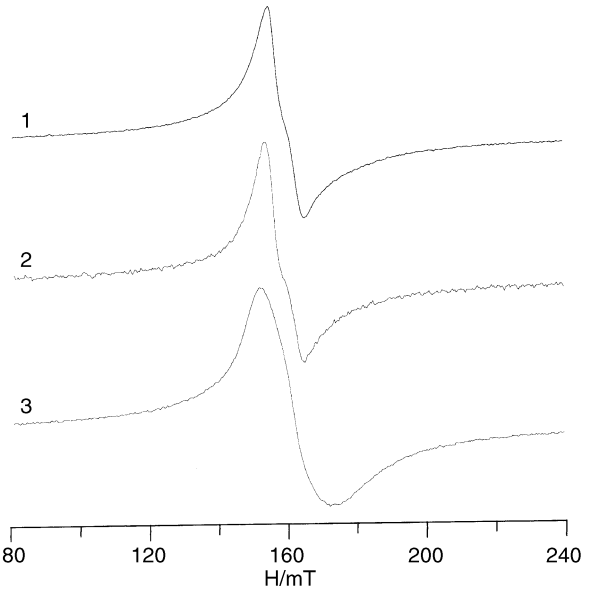

Fig. 6 ESR spectra of Fe(III)–TRENCAMS (spectrum 1), Fe(III)–TRENCAM (spectrum 2) and Fe(III)–CacCAM (spectrum 3): 1 mM concentration in 10% glycerol, 0.1 M Tris-Cl buffer, pH 7.2, T = 100 K.

salicylate coordination in $[FeLH_2]^{2-}$. Table 1 summarizes the spectral characteristics and the pK_a of several catecholate complexes and their protonated species. The first two protonation constants of the Fe(III)–CacCAM complex (6.59 and 5.15 for FeLH and $FeLH_2$) are lower than those for Fe(III)–MECAM[11] (7.02 and 6.03) but significantly higher than those for enterobactin[11] (4.95 and 3.52). The relatively high pK_a values for Fe–CacCAM reflects the stability of the bis-salicylate complex ($[FeLH_2]^{2-}$) at high pH. It should be noted that the difference between the value of pK_{FeLH_2} and pK_{FeLH} varies over the range 1.2–1.6 for the various complexes. This indicates that the equilibrium constant between the mono-$[FeLH]^{3-}$ and the bis-salicylate $[FeLH_2]^{2-}$ complexes depends very little on the tripodal backbone of the ligand.

EPR spectroscopy

The X-band EPR spectra of frozen aqueous solutions (with 10% glycerol) of iron(III) complexes of TRENCAM, TRENCAMS and CacCAM were recorded at 100 K (pH 7.2). The spectra exhibit one single dissymetric signal at a g value close to 4.3, characteristic of a high-spin octahedral ligand field with a slightly rhombic distorted geometry around the iron center. Spectra of Fe(III)–TRENCAM and Fe(III)–TRENCAMS are similar, as shown in Fig. 6 (the differential spectrum is very close to a baseline). They are both centered at $g = 4.28$. The spectrum of Fe(III)–CacCAM shows a signal centered at $g = 4.25$ with a larger linewidth than that for Fe(III)–TRENCAM. The larger linewidth may be interpreted as due to a less tightly bonded Fe(III) with CacCAM than with TRENCAM: in the former the carboxylic group is located outside of the "umbrella" of the three arms enclosing the iron atom, while in the latter the nitrogen electron pair is inside the "umbrella" of the TREN backbone and can establish hydrogen bonds with amide protons, leading to a tight cavity around the ferric ion.

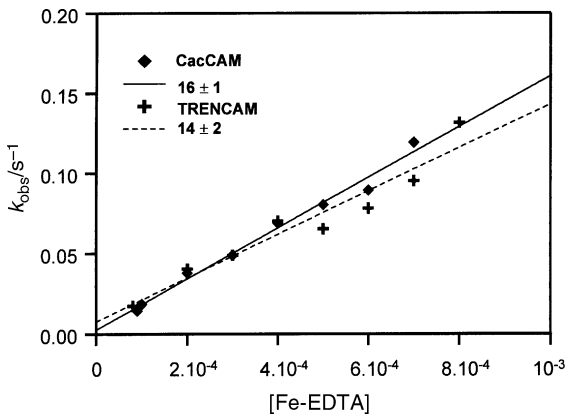

Fig. 7 Rate constants k_{obs} (s^{-1}) for iron-exchange reactions from Fe(III)–EDTA to CacCAM and TRENCAM (2% MeOH by volume): [Fe(III)–EDTA] = 0.02 mM, [CacCAM, TRENCAM] = 0.08–0.8 mM; solvent: [HEPES] = 0.05 M, I = 0.1 M ($NaClO_4$), pH 7.0, T = 25 °C.

Kinetic studies

The iron exchange between the ferric EDTA complex and CacCAM or TRENCAM has been measured at pH 7.0 (pseudo-first-order conditions with ligand concentration in excess with respect to the complex) by monitoring the increase in absorbance at 500 nm on the minute time scale. A mono-exponentional signal was observed and could be fitted to obtain the pseudo-first-order rate constants k_{obs}. The plot of k_{obs} *vs.* the ligand concentration, presented in Fig. 7, shows a linear dependence. From the slope, the second-order rate constants k_e can be calculated from:

$$d[FeL]/dt = k_{obs}[FeEDTA]_{tot} = k_e[LH_6]_{tot}[FeEDTA]_{tot} \quad (9)$$

corresponding to the global reaction:

$$FeEDTA + LH_6 \xrightarrow{k_e} FeL + YH + 5H^+ \quad (10)$$

The values of k_e are 16 ± 1 and 14 ± 2 M^{-1} s^{-1} for CacCAM and TRENCAM, respectively.

At pH 7, the reaction proceeds through four paths when taking into account the hydrolysis reaction of the ferric EDTA complex ($K_{OH} = 10^{-7.37}$)[15] and the LH_6^-/LH_5^{2-} equilibrium ($K_{a_6} = 10^{-7.19}$). The determination of the rate constants for the different paths requires the measurement of k_{obs} at various pH, but this was not done in this study. A value of 3.3 M^{-1} s^{-1} was determined under the same conditions for O-TRENSOX,[18] a tripodal ligand containing 8-hydroxyquinoline chelating units. Our results show that the exchange rate of Fe(III) between Fe–EDTA and tripodal ligands are higher for ligands with catechol groups.

Plant nutrition studies

The growth and greening of *Arabidopsis thaliana* plant cells fed with Fe(III)–CacCAM and Fe(III)–TRENCAMS as the only source of iron has been studied. In one control experiment, iron was provided with Fe(III)–EDTA and in another, no iron source was added. Results obtained for CacCAM are shown in Fig. 8 and 9. Growth and resistance to chlorosis are equivalent when Fe(III)–CacCAM or Fe(III)–TRENCAMS are used instead of Fe(III)–EDTA. The efficiency of Fe(III)–CacCAM and Fe(III)–TRENCAMS as an iron source for *A. thaliana* is good, comparable to that of Fe(III)–EDTA, the most commonly used iron source for plant nutrition.

Conclusions

The solution coordination chemistry studies described in this paper have shown that CacCAM, an analog of enterobactin, possesses properties similar to those of TRENCAM, a known and efficient iron chelator. Moreover, preliminary biological studies have shown that CacCAM possesses good efficiency for iron plant nutrition. The fact that the new C-functionalized spacer involved in the structure of CacCAM

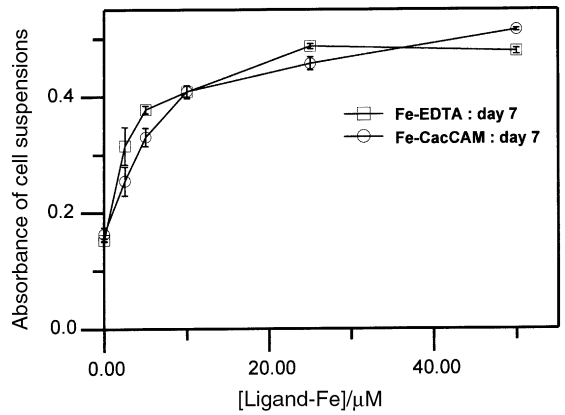

Fig. 8 Growth of *A. thaliana* cells using Fe(III)–EDTA or Fe(III)–CacCAM as siderophores: 25 °C, 220 rpm, 18 h of light per day.

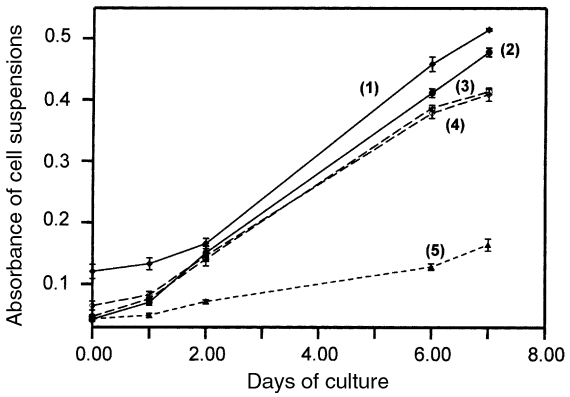

Fig. 9 Growth of *A. thaliana* cells using Fe(III)–EDTA or Fe(III)–CacCAM as siderophores. (Curve 1) 50 μM Fe(III)–CacCAM, (curve 2) 50 μM Fe(III)–EDTA, (curve 3) 10 μM Fe(III)–EDTA, (curve 4) 10 μM Fe(III)–CacCAM, (curve 5) without iron: 25 °C, 220 rpm, 18 h of light per day.

does not alter the complexing ability of the ligand (compared to the widely used TREN spacer) is very promising. The carboxylic function located outside of the coordination sphere may allow the connection of any substituent. Studies are in progress concerning (*i*) the grafting of a fluorescent probe and (*ii*) the grafting of polyoxyethylene units allowing control of the hydrophic/lipophilic balance without the help of the charged and hydrophilic sulfonate groups commonly used to confer water solubility.

Experimental

Materials and equipment

Solvents were purified by the usual techniques. All other compounds were of reagent grade and were used without further purification. Iron(III) stock solutions were prepared by dissolving appropriate amounts of ferric perchlorate hydrate (Aldrich) in standardized $HClO_4$ and $NaClO_4$ solutions. The solutions were spectrophotometrically calibrated for ferric ion by using a molar extinction coefficient of 4160 M^{-1} cm^{-1} at 240 nm.[19] IR spectra were collected on a Nicolet Impact 400 spectrometer. UV–visible absorption spectra were recorded on a Perkin–Elmer Lambda 2 spectrometer using 1.000 cm path length quartz cells and connected to an IBM PC 340 microcomputer. Mass spectra were recorded on a NERMAG 101 °C mass spectrometer. Microanalysis were performed by the Central Service of CNRS (Solaize, France). Melting points were determined with a Büchi apparatus and are not corrected. ^1H and ^{13}C NMR spectra were obtained in 5 mm tubes at 25 °C with a Bruker AM 300 spectrometer. EPR studies have been conducted using a ESP 300E Bruker apparatus with a variable temperature unit. Spectra were treated by using the WinEPR software (Bruker). Each aqueous sample (200 μL) contained 10% glycerol, 0.1 M Tris-Cl buffer, pH 7.2, 10^{-3} M Fe–CacCAM and Fe–TRENCAMS, 0.5×10^{-3} M Fe–TRENCAM. The temperature was 100 K and the field was scanned from 1000 to 5000 gauss.

Synthesis of CacCAM

4-(2-Cyanoethyl)-4-cyclohexyliminomethylheptane-1,7-dinitrile (1). Acetaldehyde (16.9 mL) was slowly added to a solution of cyclohexylamine (34.3 g, 0.3 mmol) in 15 ml of dry toluene at 0 °C, over 20 min. K_2CO_3 (2.5 g) was added and the reaction mixture was stirred for 10 min and then allowed to warm to room temperature. The organic layer was placed in an autoclave and 68.5 mL of acrylonitrile was added. The solution was stirred for 4 h at 170 °C. The black reaction mixture was cooled to −20 °C for 6 h. The crystalline product was washed with diethyl ether to give 41 g (white crystals, 48%) of **1**, which was used without further purification. Mp 99–100 °C. IR (KBr) $\nu(cm^{-1})$: 2248, 1663. ^1H NMR (300 MHz, $CDCl_3$): δ 1–2 (m, 16H, $CH_2CH_2CN + CH_2$ cyc), 2.37 (t, 6H, $J = 7.9$ Hz, CH_2CN), 3.01 (m, 1H, CH cyc), 7.45 (s, 1H, CH=N–). ^{13}C NMR (300 MHz, $CDCl_3$): δ 11.67, 29.34 (CH_2CH_2CN), 24.16, 25.26, 34.02 (CH_2 cyc), 43.07 (Cq), 69.29 (CH cyc), 119.13 (CN), 161.23 (CH).

4-(2-Cyanoethyl)-4-formylheptane-1,7-dinitrile (2). Compound **1** (10 g, 35.2 mmol) was dissolved in a solution of concentrated HCl (5 mL) and water (130 mL). The resulting mixture was refluxed for 30 min, filtered hot and allowed to cool to 0 °C. The yellow precipitate was collected, washed with water, dried and purified by recrystallisation from methanol (white crystals, 6.6 g, 92%). Mp 108 °C. IR (KBr) ν (cm^{-1}): 2250, 1716. ^1H NMR (300 MHz, DMSO-d_6): δ 1.84 (t, 6H, $J = 7.9$ Hz, CH_2CH_2CN), 2.40 (t, 6H, $J = 7.9$ Hz, CH_2CN), 9.42 (s, 1H, CHO). ^{13}C NMR (300 MHz, DMSO-d_6): δ 12.07, 26.94 (CH_2CH_2CN), 50.91 (Cq), 118.01 (CN), 200.88 (CHO).

4-(2-Cyanoethyl)-4-hydroxymethylheptane-1,7-dinitrile (3). $NaBH_4$ (1.5 g) was added to a solution of **2** (5 g, 24.6 mmol) in distilled methanol (250 mL) under nitrogen at 0 °C within 30 min. The solution was stirred for an additional 2 h at room temperature. Water (50 mL) was added and the resulting mixture was cooled to 0 °C and then acidified with concentrated HCl to pH 1. Methanol was evaporated and the product was extracted with dichloromethane (3 × 75 mL), the combined extracts were dried with Na_2SO_4. The solvent was removed to yield **3** as a white crystalline material (4.6 g, 92%). Mp 69 °C. IR (KBr) $\nu(cm^{-1})$: 3462, 2248. ^1H NMR (300 MHz, $CDCl_3$): δ 1.79 (t, 6H, $J = 7.8$ Hz, CH_2CH_2CN), 2.44 (t, 6H, $J = 7.8$ Hz, CH_2CN), 3.56 (d, 2H, $J = 3.6$ Hz, CH_2OH). ^{13}C NMR (300 MHz, $CDCl_3$): δ 11.85, 29.35 (CH_2CH_2CN), 39.59 (Cq), 65.02 (CH_2OH), 119.37 (CN). MS (DCI, NH_3 + isobutane): m/z 206 (M + 1).

4-(*tert*-Butyldimethylsilanyloxymethyl)-4-(2-cyanoethyl)-heptane-1,7-dinitrile (4). To a solution of **3** (2 g, 9.75 mmol) in freshly distilled dichloromethane (50 mL) under nitrogen, were added *tert*-butyldimethylsilyl chloride (1.62 g, 10.72 mmol), 4-dimethylaminopyridine (1.19 g, 9.75 mmol) and triethylamine (1.37 mL, 9.75 mmol). The solution was heated to reflux for 48 h, cooled, washed with brine, filtered and dried with Na_2SO_4. Evaporation of the solvent gave **4** as a white solid (2.55 g, 82%). Mp 72 °C. IR (KBr) $\nu(cm^{-1})$: 2247. ^1H NMR (250 MHz, $CDCl_3$): δ 0.04 (s, 6H, CH_3), 0.87 (s, 9H, CH_3 of Bu^t), 1.68 (t, 6H, $J = 7.8$ Hz, CH_2CH_2CN), 2.31 (t, 6H, $J = 7.8$ Hz, CH_2CN), 3.34 (s, 2H, CH_2O). ^{13}C NMR

(250 MHz, $CDCl_3$): δ −5.78 (CH_3), 25.59 (CH_3 of Bu^t), 11.75, 29.38 (CH_2CH_2CN), 17.96 (CqSi), 39.80 (Cq), 65.77 (CH_2), 119.31 (CN). MS (DCI, NH_3 + isobutane): 320 (M + 1).

4-(3-Aminopropyl)-4-(*tert*-butyldimethylsilanyloxymethyl) heptane-1,7-diamine (5). To a solution of **4** (5 g, 15.65 mmol) in 95% ethanol (60 mL) at 0 °C, were added NaOH (2.4 g, 60 mmol) and hydrazine 99% (6 mL). To this mixture Raney nickel (700 mg, 12 mmol) was added in small portions within 2 h; the solution was stirred for an additional 1 h. The reaction mixture was heated to reflux for 45 min, filtered hot and evaporated to give an oil. Addition and evaporation of toluene were repeated until NaOH precipitated. Evaporation of the filtrate gave **5** as an oil (4.77 g, 88%). IR (KBr) ν(cm^{-1}): 3375, 1607, 1442. ^{1}H NMR (300 MHz, DMSO-d_6): δ 0.01 (s, 6H, CH_3), 0.85 (s, 9H, CH_3 of Bu^t), 1.10 (m, 6H, CH_2), 1.21 (m, 6H, CH_2), 2.40 (t, 6H, J = 6.8 Hz, CH_2NH_2), 3.23 (s, 2H, CH_2O). ^{13}C NMR (300 MHz, DMSO-d_6): δ −5.82 (CH_3), 25.75 (CH_3 of Bu^t), 27.13, 30.96 (CH_2), 42.99 (CH_2NH_2), 17.93 (CqSi), 39.08 (Cq), 66.12 (CH_2O). MS (DCI, NH_3 + isobutane): m/z 332 (M + 1). Anal. calcd. (found) for $C_{17}H_{41}N_3OSi \cdot 0.25CH_2Cl_2$: C, 58.79 (58.72); H, 12.10 (11.85); N, 11.67 (11.91)%.

2,2,2-Tris[3-(2,3-dimethoxybenzamido)propyl]-*tert*-butyldimethylsilanyloxyethane (6). 2,3-Dimethoxybenzoic acid (0.91 g, 5 mmol) was dissolved in 10 mL of thionyl chloride. The reaction mixture was stirred under nitrogen for 6 h. The solution was evaporated to dryness and the residue treated with 4 × 40 mL of dry hexane. The solid residue was dissolved in freshly distilled dichloromethane (50 mL) under nitrogen. Compound **5** (0.5 g, 1.51 mmol), dissolved in a solution of freshly distilled dichloromethane (50 mL) and triethylamine (0.9 mL), was added to the solution of acid chloride within 30 min. The mixture was stirred overnight at room temperature, filtered, washed with brine and dried with $MgSO_4$ and then evaporated to dryness. The white residue was purified by column chromatography (silica gel; 1% MeOH in CH_2Cl_2). **6** was obtained as a white foamy material (0.72 g, 58%). IR (film from $CHCl_3$) ν(cm^{-1}): 3380, 1648. ^{1}H NMR (300 MHz, $CDCl_3$): δ 0.08 (s, 6H, CH_3), 0.75 (s, 9H, CH_3 of Bu^t), 1.24 (m, 6H, CH_2), 1.45 (m, 6H, CH_2), 3.25 (s, 2H, CH_2O), 3.34 (br q, 6H, J = 6.44 Hz, CH_2NH), 3.80 (br s, 18H, OCH_3), 6.94 (dd, 3H, J_1 = 8.0 Hz, J_2 = 1.6 Hz, ArH), 7.05 (t, 3H, J = 8.3 Hz, ArH), 7.58 (dd, 3H, J_1 = 8.0 Hz, J_2 = 1.6 Hz, ArH), 7.90 (br t, 3H, NH). ^{13}C NMR (300 MHz, $CDCl_3$): δ −5.61 (CH_3), 18.11 (CqSi), 23.38 (CH_2), 25.81 (CH_3 of Bu^t), 31.63 (CH_2), 39.34 (Cq), 40.49 (CH_2NH), 56.02 (OCH_3), 61.29 (OCH_3), 66.87 (CH_2), 115.15 (CH), 122.73 (CH), 124.30 (CH), 126.91 (Cq), 147.36 (Cq), 152.51 (Cq), 165.21 (C=O). MS (FAB, NBA matrix): m/z 825 $[M + 1]^+$. Anal. calcd. (found) for $C_{44}H_{65}N_3O_{10}Si \cdot CH_2Cl_2$: C, 59.35 (59.46); H, 7.40 (7.43); N, 4.57 (4.62)%.

2,2,2-Tris[3-(2,3-dimethoxybenzamido)propyl]ethanol (7). Compound **6** (0.5 g, 0.61 mmol) was dissolved in THF (10 mL) at 0 °C. Tetrabutylammonium fluoride (0.57 g, 1.8 mmol) was slowly added and the green reaction mixture was heated at reflux for 2 h. The solution was evaporated and the resulting residue was dissolved in dichloromethane, washed with brine and dried with $MgSO_4$. The orange-green residue was purified by column chromatography (silica gel; 3% MeOH in CH_2Cl_2). **7** was obtained as a white foam (0.38 g, 89%). IR (film from $CHCl_3$) ν(cm^{-1}): 3378, 2937, 1643. ^{1}H NMR (300 MHz, $CDCl_3$): δ 1.27 (m, 6H, CH_2), 1.48 (m, 6H, CH_2), 3.34 (m, 8H, CH_2NH + CH_2O), 3.79 (br s, 18H, OCH_3), 6.92 (dd, 3H, J_1 = 8.0 Hz, J_2 = 1.6 Hz, ArH), 7.07 (t, 3H, J = 8.0 Hz, ArH), 7.65 (dd, 3H, J_1 = 8.0 Hz, J_2 = 1.6 Hz, ArH), 7.96 (br t, 3H, NH). ^{13}C NMR (300 MHz, $CDCl_3$): δ 23.20 (CH_2), 31.08 (CH_2), 39.34 (Cq), 40.37 (CH_2NH), 55.95 (OCH_3), 61.23 (OCH_3), 66.14 (CH_2O), 115.09 (CH), 122.61 (CH), 124.25 (CH), 126.79 (Cq), 147.29 (Cq), 152.45 (Cq), 165.19 (C=O). MS (FAB, NBA matrix): m/z 711 $[M + 1]^+$. Anal. calcd. (found) for $C_{38}H_{51}N_3O_{10} \cdot 1.25CH_2Cl_2 \cdot 0.75MeOH$: C, 57.16 (57.19); H, 6.57 (6.78); N, 4.83 (4.99)%.

2,2,2-Tris[3-(2,3-dimethoxybenzamido)propyl]ethanal (8). A solution of dimethyl sulfoxide (51 μL, 0.66 mmol) in dry dichloromethane (150 μL) was added to a solution of oxalyl chloride (30 μl, 0.33 mmol) in freshly distilled dichloromethane (1 ml). The mixture was stirred for 5 min and then a solution of **7** (0.21 g, 0.3 mmol) in dry dichloromethane (200 μL) was added within 2 min; the solution was stirred for an additional 15 min. Triethylamine (420 μL, 3 mmol) was added and the reaction mixture was allowed to warm to room temperature. Water (20 mL) and dichloromethane (50 mL) were added and the organic layer was washed with brine and dried with $MgSO_4$. The solvent was removed and the yellow residue was purified by column chromatography (silica gel; 1% MeOH in CH_2Cl_2). **8** was obtained as a white foam (0.17 g, 82%). IR (film from $CHCl_3$) ν(cm^{-1}): 3380, 2939, 1721, 1651. ^{1}H NMR (300 MHz, $CDCl_3$): δ 1.48 (m, 6H, CH_2), 1.59 (m, 6H, CH_2), 3.34 (br q, 6H, CH_2), 3.79 (br s, 18H, OCH_3), 6.90 (dd, 3H, J_1 = 8.1 Hz, J_2 = 1.6 Hz, ArH), 7.07 (t, 3H, J = 8.0 Hz, ArH), 7.56 (dd, 3H, J_1 = 8.1 Hz, J_2 = 1.6 Hz, ArH), 7.94 (br t, 3H, NH), 9.37 (s, 1H, CHO). ^{13}C NMR (300 MHz, $CDCl_3$): δ 24.22 (CH_2), 32.06 (CH_2), 40.01 (CH_2NH), 48.21 (Cq), 56.1 (OCH_3), 61.42 (OCH_3), 115.39 (CH), 122.79 (CH), 124.22 (CH), 126.83 (Cq), 147.48 (Cq), 152.41 (Cq), 165.38 (C=O amide), 201.05 (C=O aldehyde).

2,2,2-Tris[3-(2,3-dimethoxybenzamido)propyl]acetic acid (9). Compound **8** (158 mg, 0.22 mmol) was dissolved in THF (3 mL) and water (3 mL). Sulfamic acid (H_2NSO_3H, 29 mg, 0.29 mmol) was added, the solution was stirred for 5 min and then sodium chlorite ($NaClO_2$, 26 mg, 0.29 mmol) was added. The reaction mixture was stirred for 1 h at room temperature. CH_2Cl_2 (40 mL) and water (50 mL) were then added and the organic layer was washed with water and dried with $MgSO_4$. The solvent was removed and the white residue was purified by column chromatography (silica gel; 4% MeOH in CH_2Cl_2). Evaporation of the eluant gave **9** as a white foam (145 mg, 90%). ^{1}H NMR (300 MHz, $CDCl_3$): δ 1.48 (m, 6H, CH_2), 1.59 (m, 6H, CH_2), 3.35 (br q, 6H, CH_2), 3.79 (br s, 18H, OCH_3), 6.91 (dd, 3H, J_1 = 8.1 Hz, J_2 = 1.6 Hz, ArH), 7.01 (t, 3H, J = 8.0 Hz, ArH), 7.54 (dd, 3H, J_1 = 7.9 Hz, J_2 = 1.6 Hz, ArH), 7.97 (br t, 3H, NH). ^{13}C NMR (300 MHz, $CDCl_3$): δ 24.33 (CH_2), 32.1 (CH_2), 40.22 (CH_2NH), 48.29 (Cq), 56.05 (OCH_3), 61.39 (OCH_3), 115.37 (CH), 122.77 (CH), 124.99 (CH), 126.72 (Cq), 147.52 (Cq), 152.55 (Cq), 165.41 (C=O amide), 177.09 (CO_2H). MS (FAB, NBA matrix): 725 $[M + 1]^+$. Anal. calcd. (found) for $C_{38}H_{49}N_3O_{11} \cdot CH_2Cl_2$: C, 58.20 (57.92); H, 6.42 (6.36); N, 5.28 (5.20)%.

2,2,2-Tris[3-(2,3-dihydroxybenzamido)propyl]acetic acid (10). To a solution of **9** (0.2 g, 0.28 mmol), dissolved in freshly distilled dichloromethane and cooled to 0 °C under nitrogen, was added a solution of BBr_3 in dichloromethane (1 M, 5 mL). The yellow suspension was stirred overnight at room temperature. Methanol was added and the solvents were evaporated. Addition and evaporation of methanol were repeated five times. The residue was applied to a Sephadex LH-20 column (50% MeOH–CH_2Cl_2). A white product, eluted as a single band, was obtained (138 mg, 78%). ^{1}H NMR (300 MHz, DMSO-d_6): δ 1.45 (m, 12H, CH_2), 3.23 (br q, 6H, CH_2NH), 6.66 (t, 3H, J = 8.01 Hz, ArH), 6.88 (dd, 3H, J_1 = 8.0 Hz, J_2 = 1.2 Hz, ArH), 7.24 (dd, 3H, J_1 = 8.0 Hz, J_2 = 1.2 Hz, ArH), 8.79 (t , 3H, J = 5.4 Hz, NH), 12.84 (br s, 1H, CO_2H). ^{13}C NMR (300 MHz, DMSO-d_6): δ 23.75 (CH_2), 31.49 (CH_2), 39.37 (CH_2NH), 48.51 (Cq), 114.8 (Cq), 117.05 (CH), 117.88 (CH), 118.76 (CH), 146.20 (Cq), 149.75 (Cq),

169.70 (C=O amide), 177.68 (CO_2H). MS (FAB, NBA matrix): m/z 641 $[M+1]^+$. Anal. calcd. (found) for $C_{32}H_{37}N_3O_{11}\cdot 0.75CH_2Cl_2\cdot 0.25MeOH$: C, 55.70 (55.72); H, 5.85 (5.60); N, 6.19 (5.91)%.

Potentiometric experiments

All the measurements were made at 25 °C in deionized and twice-distilled water. The ionic strength was kept constant at 0.1 M (sodium perchlorate, PROLABO, Puriss). Due to the low solubility of the ligand in water, 2% MeOH was added. Such a low ratio of MeOH does not change significantly the solvent properties[7] and thus the measured pH values were not corrected. The potentiometric titrations were performed using an automatic titrator system, DMS Titrino (Metrohm), with a combined glass electrode (Metrohm filled with NaCl saturated solution) and connected to an IBM Aptiva microcomputer. The electrodes were calibrated to read the pH according to the classical method.The ligand and its iron(III) complex (0.5 mM) were titrated with standardized 0.02 M NaOH. Argon was bubbled through the solutions to exclude CO_2 and O_2. Carbonate content was checked by Gran's method. The titration data (106 points, pH range 6.0–10.6) were refined by the nonlinear least squares fitting program SUPERQUAD[9] to determine the ligand deprotonation constants.

Spectrophotometric measurements

The temperature was maintained at 25 °C with a variable temperature unit Perkin–Elmer PTP-1 and the acquisition was made with the UV Winlab software (Perkin–Elmer). The ionic strength has been kept constant at 0.1 M (sodium perchlorate and pH buffer when indicated). Methanol (2%) was added for ligand titration and kinetic measurements. pH measurements were made with a 713 Metrohm digital pH meter equipped with a microelectrode. The titration data were analysed using the nonlinear least squares fitting program LETAGROP SPEFO.[13,14] The calculations were performed using absorbance values at 10 wavelengths and the residual square sums of the fit were 10^{-3}. In order to determine β_{110}, a competition with EDTA was carried out for one week in the dark at 25 °C (HEPES buffer). Kinetic data were saved in ASCII format; from these, Biokine ASCII files were built. These data were treated by using the BIOKINE 3.02 software (BIO LOGIC Co., Claix, France).

Cell culture and growth measurement

Plant cells were grown in 24-well sterile cell culture plates (Nunc); each independent axenic culture contained 1.5 ml of culture medium. This was a modified Murashige and Skoog (MS) medium:[20] for 1000 ml of medium 4.3 g macro and micro elements powder (provided by Duchefa, catalog number M0221, Haarlem Netherlands), 10 ml H_2KPO_4 (20 g l^{-1}), 0.5 ml Kinetin (0.1 g l^{-1}), 0.5 ml of (2,4-dichlorophenoxy) acetic acid (0.2 g l^{-1}); 1 ml of vitamin solution (Duchefa M 0409) and 30 g saccharose. The complex Fe(III)–CacCAM was first prepared at low pH then raised to pH 5.8 with NaOH and a tris-maleate buffer. Wells were inoculated at an absorbance of 0.003 ($\sim$1/12) with early stationary phase *Arabidopsis thaliana* (var. Columbia) cell suspension. For axeny, plates were sealed with Magic Scotch™ tape. 24-Well plates were agitated at 220 rpm at 25 °C in a New Brunswik Innova 4230 refrigerated incubator shaker. Light was supplied 18 h a day by two Sylvania Growlux 15-watt bulbs in the photosynthesis accessory.

The measurements of cell density were made daily. It was often hampered by the occurrence of condensation droplets on the cover of the 24-wells plates. To minimize light scattering during densitometry, the numerized images of the cultures were recorded from beneath through a mirror. The Bio-Rad video camera system Geldoc 1000 was used, with the molecular analyst software for quantification. To record images of the plates, the hood of the camera was rotated to a horizontal position. A mirror was introduced through the open door of the hood, at 45° across the horizontal light path, held by a special stand, which also maintained the 24-well culture plate horizontally on a glass plate and held the Geldoc light source, upside 10 cm above the cultures. Full frame images were captured under constant light conditions, that is the white light being adjusted so that just a few saturated pixels appeared in red in the empty optical field. Under these light conditions, a reproducible relationship was found between the absorbance of wells in densitometric scanning profiles of recorded images and the amount of cells in the wells. Images of culture plates without cells were used as baseline reference. They showed an uneven light background. This fact was compensated by the subtraction of an adapted baseline. Measurements and baseline profiles were drawn using the rectangle tool of the image analysis software. Baselines were drawn by joining the crest highlight points in each image between the wells and then subtracted. This method was found to be more accurate and reproducible than the use of 24 grids, or the elliptical objects tools proposed by the software.

References

1 J. B. Neilands, *J. Biol. Chem.*, 1995, **270**, 26723.
2 G. S. Tilbrook and R. C. Hider, in *Iron Transport and Storage in Microorganisms, Plants and Animals*, ed. A. Sigel and H. Sigel, M. Dekker, New York, 1998, ch. 18, p. 691.
3 C. Caris, P. Baret, C. Béguin, G. Serratrice, J.-L. Pierre and J.-P. Laulhère, *Biochem. J.*, 1995, **312**, 879.
4 A. Shanzer and J. Libman, in *Iron Transport and Storage in Microorganisms, Plants and Animals*, ed. A. Sigel and H. Sigel, M. Dekker, New York, 1998, ch. 8, p. 329.
5 A. M. Albrecht–Gary and A. L. Crumbliss, in *Iron Transport and Storage in Microorganisms, Plants and Animals*, ed. A. Sigel and H. Sigel, M. Dekker, New York, 1998, ch. 7, p. 239.
6 F. Thomas, P. Baret, D. Imbert, J.-L. Pierre and G. Serratrice, *Bioorg. Med. Chem. Lett.*, 1999, **9**, 3035.
7 S. J. Rodgers, C. W. Lee, C. Y. Ng and K. N. Raymond, *Inorg. Chem.*, 1987, **26**, 1622.
8 F. Thomas, C. Béguin, J.-L. Pierre and G. Serratrice, *Inorg. Chim. Acta*, 1999, **291**, 148.
9 P. Gans, A. Sabatini and A. Vacca, *J. Chem. Soc., Dalton Trans.*, 1985, 1195.
10 T. M. Garrett, P. W. Miller and K. N. Raymond, *Inorg. Chem.*, 1989, **28**, 128.
11 L. D. Loomis and K. N. Raymond, *Inorg. Chem.*, 1991, **30**, 906.
12 Z. Hou, T. D. P. Stack, C. J. Sunderland and K. N. Raymond, *Inorg. Chim. Acta*, 1997, **263**, 341.
13 L. G. Sillen and B. Warsquist, *Ark. Kemi*, 1969, **31**, 377.
14 M. Meloun, J. Havel and E. Hogfeldt, *Computation of Solution Equilibria*, Ellis Horwood, Chichester, 1988.
15 R. M. Smith and A. E. Martell, *Critical Stability Constants*, Plenum Press, New York, 1989, vol. VI.
16 A. Ringbom, *Complexation in Analytical Chemistry*, Interscience, New York, 1963.
17 W. R. Harris, K. N. Raymond and F. L. Weitl, *J. Am. Chem. Soc.*, 1981, **103**, 2667.
18 H. Boukhalfa, Ph.D. thesis, Université de Grenoble, 1996.
19 R. Bastian, R. Weberling and F. Palilla, *Anal. Chem.*, 1956, **28**, 459.
20 T. Murashige and F. Skoog, *Physiol. Plant.*, 1962, **15**, 473.